Proton Proton Collisions at the LHC and Future Colliders

Paul Kothgasser

A thesis submitted in partial fulfillment
of the requirements for the degree of
Bachelor of Science - Bsc
in Physics
University of Graz

Supervisor
Univ.-Prof. Dipl.-Phys. Dr.rer.nat. Axel Maas
Co-Supervisor
Dipl.-Phys. Dr.rer.nat. Simon Plaetzer

Institute of Physics November 21, 2023

Inhaltsverzeichnis

1 Abstract

The following thesis compares how changing the coupling between the Higgs (h_0) and Z or Higgs and $W^{\pm}$ boson affects the simulated event flow at a simulated Large Hadron Collider (LHC) event. In the following, the placeholder V will be used to refer to either of the vector bosons Z or W. The interactions were incorporated by a variation of values for their respective coupling strength. A factor representing Beyond the Standard Model (BSM) effects (FMSA) was varied independently as well. FMSA is a factor related to the treatment of bosons as particles with a non-vanishing radius section 4.5. In order to simulate events the Herwig event simulator [4] was used and plots of relativistic invariant values generated using rivet [5] (a particle physics analysis toolkit).

2 Introduction and Outlook

The standard model (SM) is a collection of quantum field theories (QFTs) which covers the basis of modern particle physics. It describes three of the four fundamental forces (Electromagnetic, Weak and Strong) as well as all known elementary particles. The SM was discovered in stages, beginning in the later half of the 20th century and even today new research is done on it. The latest addition of a fundamental particle was that of the Higgs boson in 2012, when experiments at the CERN particle collider proved its existence. However, the model is not complete as there are phenomena which cannot be explained yet, such as: the matter antimatter asymmetry, spontaneous symmetry breaking, gravity and the connection of quantum physics and relativity.

The model still is excellent at describing more everyday processes such as particle interactions, electromagnetism, quantum mechanics and relativity (the last two only separately at the present time). To attempt and find BSM physics is quite difficult, as we do not have the capabilities to set up experiments for testing many BSM hypothesis. Some of the more common BSM theories are expressed by either varying the coupling between the Higgs boson and other bosons, or by adding in a new parameter, which the coupling is dependant on.
In this thesis, the second modification is looked at in greater detail. Specifically, unlike the SM presumption of a boson as point-like particle, this thesis explores the effects of it possessing a non-zero radius. The precise relationship between the FMSA factor and the boson radius is derived in chapter 3 of [17]. For this work, it is sufficient to note it is proportional to the square of the boson radius $< r^2 >$. The effects arising from this treatment are also briefly compared to a variation of SM couplings to see whether differentiation between the two schemes is possible.

The most accessible way of testing the limits of the SM are experiments at CERN. Since access to these facilities is limited, a different method was devised to help with the search for BSM physics. This was the use of computers for simulating events through so called "event generators". Besides the ability to run them on any computer (depending on complexity of the event), another advantage was that any SM parameters could be changed, left out or even new parameters added to the programs to further see what effects these changes would have on the events.
The simulation program used for this thesis is called Herwig and operates based on Monte Carlo Integration (an integration scheme based on random numbers). It performs additional sanity checks by calculating conserved quantities, such as Ward-Takahashi identities, and checking the deviation of the final output values from the expected ones.

The problem this thesis handles is explained in section 3 in further detail. This section also gives a short overview of the used techniques, processes and diagrams. Next section 4 covers the Herwig event generators programs, files and values which were used to generate data via simulations. Going into further detail, section 5 first discusses jet finding algorithms in general, then the choice one used in Herwig. Afterwards section 6 covers the output of the simulation. Finally section 7 gives a summary of the work and results as well as talking about potential future research.

3 Basics

The SM interactions follow a gauge theory, thus the Lagrangian is invariant under local transformations. The gauge bosons are force carriers of the SM. The ones included in the simulation are the $W^{\pm}$ and Z bosons, which mediate the electroweak force. The $W^{\pm}$ boson carries +1 or -1 times the elementary electric charge e while the Z boson is electrically neutral. The last particle of interest, which can decay into any of the three V bosons, is the scalar Higgs boson.
In the SM the decay of a Higgs boson into a V boson is treated via perturbation theory (PT) and Monte-Carlo integration techniques. Should the bosons however extend into space, then the calculation would require an augmented perturbation theory (APT), instead of relying on just the basic techniques formulated for point-like particles.

3.1 Higgs production and decay

At the LHC, SM production of the Higgs boson is dominated by the gluon fusion process gg → H (ggF)[...]. Associated production with a W boson q $\bar{q}$' → WH (WH), a Z boson q $\bar{q}$/gg → ZH (ZH) or with a pair of top quarks q$\bar{q}$/gg → t$\bar{t}$H (ttH) have sizeable contributions as well. The WH and ZH production processes are collectively referred to as the V H process. [...] Together they account for approximately 88% of all decays of a SM Higgs boson at $m_H \sim 125$ GeV.[2]

Due to its unstable nature, a Higgs boson is not in itself an observable, instead it decays into other particles (which in turn decay further) through various decay channels. Inside the input file for these simulations a decay to a tauon and an anti-tauon was the selected option. These two particles were further set to be stable, thus the constraint to two outgoing jets.

3.2 Feynmann diagrams

In the field of quantum mechanics, when dealing with particle decay and creation, often high numbers of long winded integrals pop up. To give a simplified depiction, which is more easily readable by humans, quantum mechanics and QFT often utilize pictorial representations of the underlying mathematical structure. These can each be traced back to their mathematically rigorous integral counterpart. One such structure are Feynmann diagrams, describing the space-time-evolution of a set of particles. This section will give a short overview of how to read Feynmann diagrams.

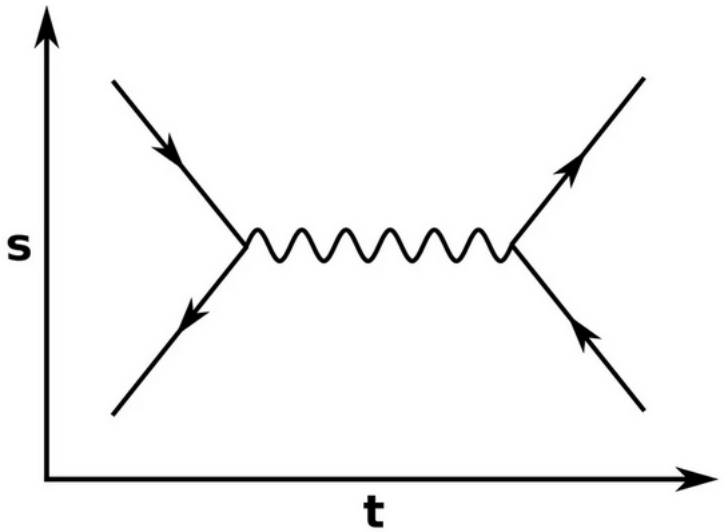

Fig. 1: A simple Feynmann diagram, s ... space axis, t ... time axis

3.2.1 Axes

In quantum field theory (QFT) space and time can no longer be treated as unrelated coordinates. A distinction is still kept, as the sign of a time-like variable is flipped to that of the three space-like ones. The time axis is multiplied by the speed of light c, so the physical units of any of the four variables are the same (length). Further in QM and QFT it is practice to use natural units such that $c = \hbar = 1$. The space-like coordinate axis in a Feynmann diagram (going from the bottom to the top here) is denoted by s while the time-like one (left to right) gets a t. Thus a Feynmann diagram shows the space-time evolution. It is however important to remember, that this matter is no longer as simple as viewing this diagrammatic depiction like a classical event, with time flowing and particles moving through space in an unrelated manner.

3.2.2 Lines and Vertices

Within the diagrams, different types of lines are used for different particle classes: full, straight lines for fermions, wiggly lines for photons and V bosons, loops for gluons and dotted lines for the Higgs boson (so far the only discovered scalar boson). Further, any point at which two (real or virtual) or more particles meet is denoted by a dot and called vertex. These vertices are the points at which interactions happen.
While the in- and out-going particles would have a vertex at their ends in momentum space, calculations involving

Feynmann diagrams usually take place in momentum space, achieved by a fourier transformation. In momentum space, as there is no fixed position, such end point vertices are missing.
On straight lines there is also an arrow, denoting the direction of the fermion-number flow. A regular particle moves in the direction of fermion flow, while a particle which moves antiparallel to it is identified as an antiparticle.
Finally a loop inside a Feynmann Diagram is a structure representing particle interactions. These can occur between different particles or a particle may affect itself (self-interaction). Loops are closed structures and can be thought to represent the exchange of virtual particles.

3.2.3 Decay Channel Diagrams

The following image shows an exemplary Feynmann diagram for associated Higgs V boson production via the s-channel:

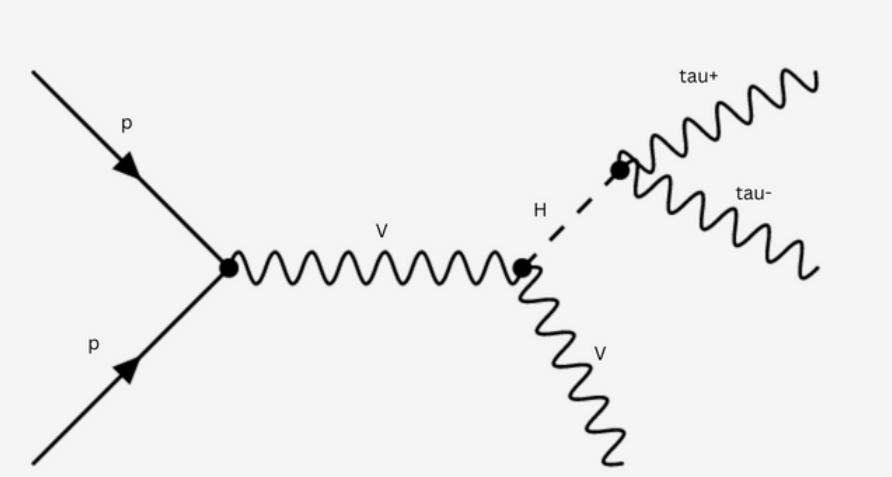

Fig. 2: Higgs decay through V bosons

In a physical event, the tauons would then go on to decay further. However, those channels are not of interest for the process being looked at here. Accordingly, the $\tau^+\tau^-$ have been set as stable particles in the simulation, to save computation time, so they don't decay any further. The following images show a simplified depiction of production and decay channels for a Higgs boson.

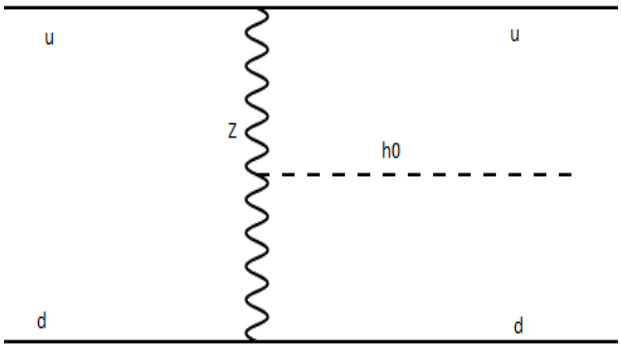

(a) Higgs boson decay via s channel and Z boson
u ... up quark, d ... down quark, Z ... Z gluon, h_0 ... Higgs boson

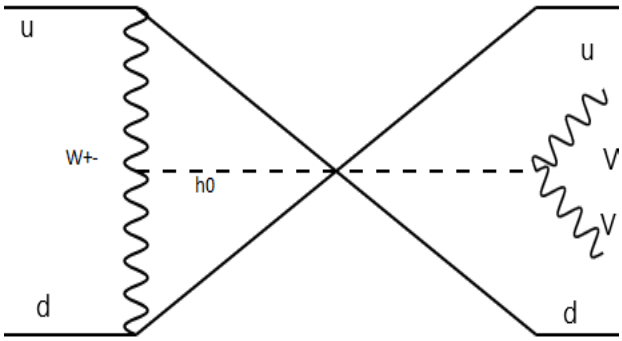

(b)
u ... up quark, d ... down quark, $W^{\pm}$ ... W gluon, h_0 ... Higgs boson, V ... vector boson

Fig. 3: example diagrams for Higgs boson decay

3.3 Higgs boson

According to current physical theories, every quantum mechanical particle is also a wave (excitation) in a field just as much as being a particle. The Higgs field was proposed in 1964 as a field permeating the universe, giving mass to elementary particles. The Higgs boson is then, according to one viewpoint, a wave in this field. [18].

The theory behind the Higgs Field was first published by Peter Higgs in [13]. The Higgs Field helped circumvent the issue, that the theory for weak interaction did not allow massive particles, yet the V bosons had to be massive in order to be consistent with the short range of the weak interaction. Through selecting one of the eigenvalues of the potential term in the Lagrangian (gauge fixing), the particles are assigned a mass term due to the broken symmetry of the system. [19].
The Higgs boson was first experimentally discovered on the 4th of July 2012 at CERN [8]. It was not possible to directly observe the Higgs particle, instead products of the particles produced in the various Higgs decay channels were measured. Indeed, even those particles did not always live long enough to reach detectors and decayed further. This process is also known as branching. From these so called "showers" of particles, that can be measured directly, a jet reconstruction algorithm scheme is applied to get an idea of the most probable original event structures ordered by their likelihood as origins of the measured final data.
The measurable particles the Higgs decays into are also produced by a plethora of different processes inside the particle collider, thus additional constraints are applied to jet finding algorithms to filter out noise. However, after a sufficient amount of collision events, the invariant mass (sum of total energy and momentum, invariant under Lorentz transformation) of some jets was equal to the proposed Higgs mass range (125 ± 0.37 GeV in natural units) [14].
As the coupling of the Higgs Field is what gives particles their mass, it couples more strongly to particles the higher their mass is.

3.3.1 first discovery of the Higgs boson

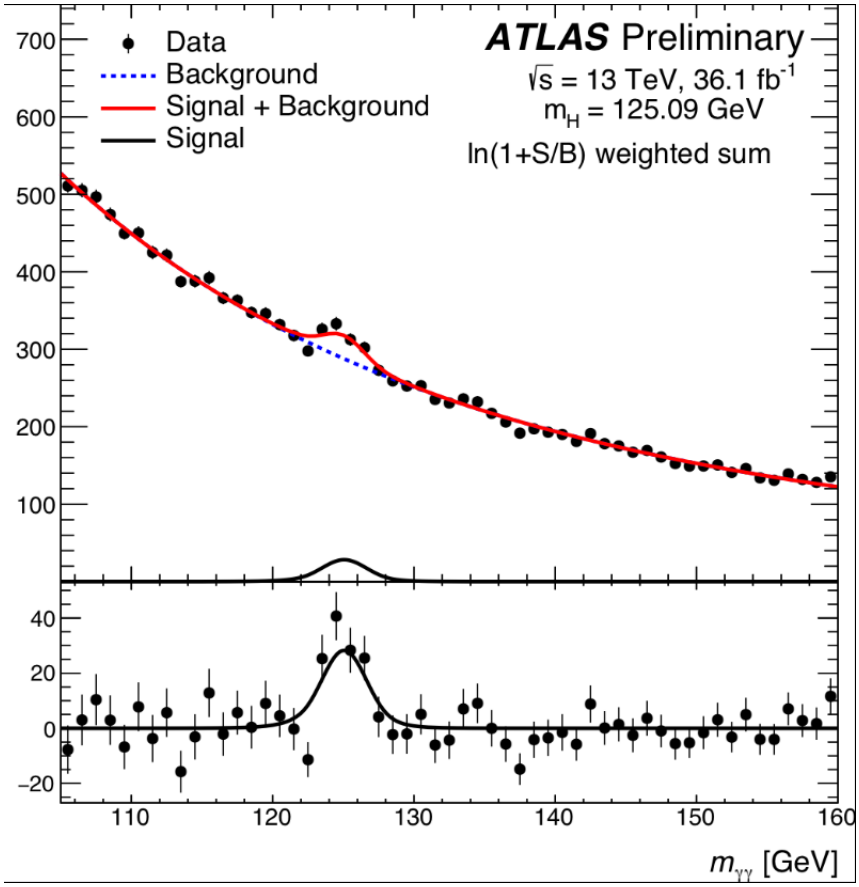

Fig. 4: mass peak at the presumed Higgs boson mass

fig. 4 gives an overview of what the original discovery graph looked like. Against the falling background spectrum (top graph of the figure) a notable peak around roughly 125 GeV of mass was discovered. After checking whether this was due to an experimental error or some other measurement issue, which yielded no results, the data was accepted to be a genuine measurement.
After normalizing the peak against background data (second and third graph) the relativistic mass of this new particle was close to the proposed mass of the Higgs boson.

3.3.2 selected decay channel

Due to its large event rate of 6.3%, the process selected for the simulation was the $h_0 -> \tau^+\tau^-$ decay [3].

3.4 Perturbation Theory

3.4.1 Basics of PT

From classical quantum mechanics, it has already been derived that the scattering amplitude or cross section between two particles (k and k') is equal to the expectation value of the Hamiltonian $< k| \mathrm{H} |k' >$. Often it is not feasible to calculate the Hamiltonian exactly and thus PT is introduced, to get a good estimate of the behavior of the system. An initial Hamiltonian H_0 is introduced, which can be calculated exactly. Next, a small perturbation λV is introduced, with λ being a sufficiently small parameter and V an operator, describing the imbalance of the system, which shifts the Hamiltonian. This new operator, consisting of H_0 and $\lambda\mathcal{V}$ is then diagonalized. After completing such a process, and comparing the resultant Hamiltonian with the original H_0, one arrives at the first order ($\mathcal{O}(1)$) energy correction. Corrections can be expanded upon in λ to higher degrees for more precise results. However, this comes at the cost of exponentially increasing computing requirements. PT works if the perturbation diverges slow enough, so that the product with λ still vanishes. In QFT, convergence is not always assured at higher orders. As the results produced so far have been in agreement with the experiment, the technique is still used prominently.

3.4.2 PT in Quantum Chromodynamics (QCD)

As we can only measure the initial and final particle flow in any experiment, there is an infinite number of possible Feynmann diagrams to calculate. The simplest form, also called tree-level or leadon order (LO), of this diagram includes only the ingoing and outgoing particles and is constrained to the least amount of internal loops for which the event could occur.
There may be any number of internal interactions, which cancel out before the final state and aren't detectable though. Depending on the amount of particles involved and how convoluted the self-interaction terms become, they are called next-to-leading-order (NLO), next-to-next-to-leading-order and so on. The diagram calculation is then associated with a variable called order $\mathcal{O}$, referring to the highest order of diagram included. These additional diagrams are treated as perturbations in PT, with the added caveat that it isn't always possible to know whether they converge a priori. The higher $\mathcal{O}$ is, the more precise the result. On the other side, computation time rises exponentially and including one more order of diagrams could lead to a tenfold increase in required time.

3.4.3 Propagator

In the realm of QFT, the Propagator or two-point function of a system is denoted by the symbol $\Delta(x-y)$. It gives the probability, that a particle which is initially at point x in hyperspace travels to point y. Propagators are often evaluated in poition space, achieved by fourier transforming the original momentum space expression. The evaluation of such a term in a Feynmann diagram is simply the line connecting two dots. As such a virtual particle could be thought of as equivalent to a propagator function. An example for the form of a propagator in QFT is that of a fermion propagator:

$$D(x-y) = \int \frac{d^4P}{(2\pi)^4} \frac{P_\mu \gamma^\mu + m\mathbb{1}}{P^2 - m^2 + i\epsilon} e^{-iP_\mu(x^\mu - y^\mu)} \tag{1}$$

with P as the momentum, $A_\mu A^\mu$ denoting a co- or contravariant tensor, γ being a gamma matrix and finally ϵ an infinitesimal value. The inclusion of ϵ avoids problems at poles and is taken to the limit of 0^+ afterwards.
In Herwig, this propagator is hardcoded into the input file used for a simulation. In the creation of this thesis, the q^2 term was the sum of q_1^2 and q_2^2, which are any pair combination of a V boson. (A Higgs to boson decay may yield singular bosons, for example an individual Z boson, but such contributions are negligible in comparison to the decay probability into pairs. As such, in the scope of this thesis only pair production is looked at).

3.5 Hadronization

Hadrons are subatomic particles of 2+ quarks, held together by the strong force, which may also interact weakly. They form out of gluons and quarks. There are two main processes by which this happens:

- quark gluon plasma (Cluster model)
- colour string decay (Lund string model)

Herwig is based on the cluster model. It's based on three main steps. First Quarks and gluons are grouped into colour-neutral clusters. While accounting for soft and hard gluon radiation, the clusters are evolved before finally hadronizing into observable hadrons through combination and recombination.

The top quark does not hadronize, as its mean lifetime (estimated at $5 \times 10^{-25} s$) is smaller than the timescale required for strong interactions to occur by an order of 10. [9], Further, as the invariant mass of the top quark is higher than that of the Higgs boson, it cannot be created from a decay of this particle.

4 Herwig

The Herwig event simulator allows it's user to simulate events based on real life experiments at the LHC. It is further possible to change some SM values to different ones, set by a different model. The event workflow is simulated via Monte-Carlo integration and can be adapted to show the outcome of LHC experiments under the adapted theory. It is then possible to compare the thus generated data with the one gained by setting all values set to their SM estimation to see how well the model works in contrast with current mainstream models of particle physics.
Another option is to simulate BSM physics in an attempt to figure out new ideas and hypotheses in the realm of particle physics.

4.1 Introduction to Herwig

Herwig is an open-source software package based on python, C++ and Linux scripts. It can be downloaded using a bootstrap script or by installing the individual options via terminal in linux. The website `https://herwig.hepforge.org/` gives detailed instructions on how to start with either option. At the time this thesis is written, the Herwig 7.0 version was used to generate data.

4.2 Herwig manual

As of the writing of this thesis November 21, 2023 the manual for the Herwig 7.0 release has not yet been published. As such, per the recommendation found on the Herwig homepage, I will refer to the Herwig++ user manual and, if necessary, the release notes.
Herwig++ is based on ThePEG — the Toolkit for High Energy Physics Event Generation, a framework for implementing Monte Carlo event generators. ThePEG provides all parts of the event generator infrastructure that do not depend on the physics models used as a collection of modular building blocks. The specific physics models of Herwig++ are given on top of these.

Each part of Herwig++ is written as a C++ class that contains the implementation of the Herwig++ physics models, inheriting from an abstract base class in ThePEG. This allows the implementations of different physics models to live side-by-side and be easily exchanged. The central concept in ThePEG is the Repository, which holds building blocks in the form of C++ objects that can be combined to construct an EventGenerator object, which in turn will be responsible for all steps of event generation. Within the Repository, one can create objects, set up references between them, and change all parameter values. The Repository object needs to be populated with references to all required objects for the physics models used at run time. The objects can then be persistently stored, or combined to produce an EventGenerator. [...][1]

4.3 Herwig workflow

The EventGenerator object is responsible for the run as a whole. It holds the infrastructure objects that are needed for the run, like the generation of random numbers, the particle properties stored as ParticleData objects, and handles any exceptions. The actual generation of each event is the responsibility of the EventHandler. It manages the generation of the hard scattering process3 and the subsequent evolution of the event through five StepHandler objects, each of which is responsible for generating one main part of the event:

- The SubProcessHandler, responsible for generating the hard sub-processes.
- The CascadeHandler which generates the parton showers from them.

[1] https://arxiv.org/pdf/0803.0883.pdf

- The MultipleInteractionHandler produces additional hard scattering events when using a multiple parton-parton scattering model to simulate the underlying event in hadron-hadron collisions
- The HaronizationHandler which generates hadrons from the leftover gluons and quarks after the shower.
- The DecayHandler which decays any unstable particles.

[2]

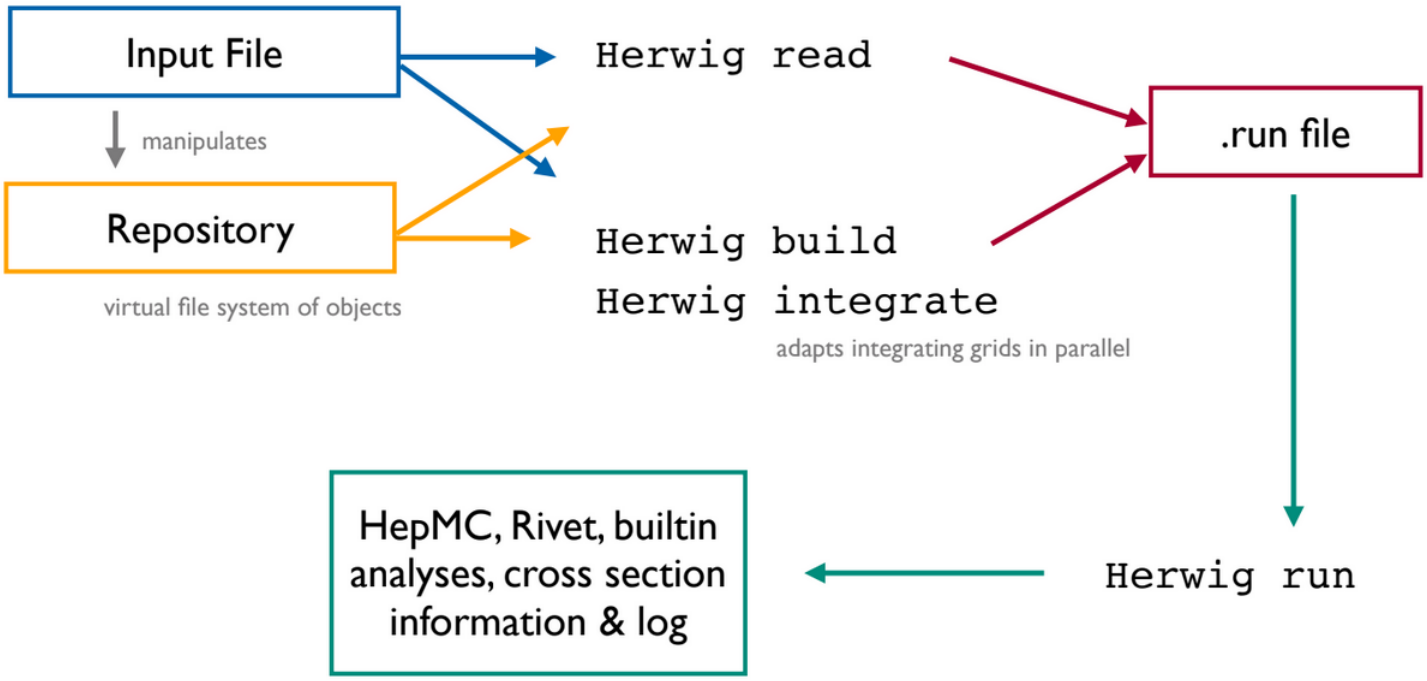

Fig. 5: Herwig workflow diagram

The usage of herwig is split into several steps, as outlined below.

[2] https://arxiv.org/pdf/0803.0883.pdf

4.3.1 Input File

First an input file is read, which provides the necessary environment data for the simulation. The file contains input settings that can be set by the user to control various aspects of the simulation. It may even contain additional processes, not built into the standard Herwig event workflow. This can be useful for adding new physics or adjusting the simulation parameters to better match experimental data. Besides those it usually contains references to the preinstalled Herwig libraries, which are used as base setup and modified according to the input file script. This step includes integrating any changes to values or files specific to the run. After completion, a .run file is generated.
As this step sets up the environment as necessary, it is possible to have set up a small amount of events for the following run, to save time. After this, there is no longer a need to set up anything and the run file can be called directly with any number of events.
The input file used in this thesis consists of the following lines: As an overview, the relevant choices are shown in the following list:

- 13 TeV for the Luminosity (ratio of detected events per time unit, over a given cross section)
- OrderinAlphaS 0 (up to how many corrections is the strong coupling constant calculated)
- OrderinAlphaEW 3 (up to how many corrections is the electroweak coupling constant calculated)
- do Factory Process p p → j j h0 (which particle interactions occur)
- JetCuts:JetRegions 0 FirstJet (pseudorapidity and transverse momentum for where to identify jets)
- JetCuts:JetRegions 1 SecondJet
- set FirstJet:PtMin 15*GeV (minimum of transverse momentum to be identified as a jet)
- set SecondJet:PtMin 15*GeV
- set JetFinder:ConeRadius 0.4
- fixed MatrixElement scale at 80 GeV
- MCatLO-DefaultShower.in (run monte carlo integration at leading order)
- Decay Modes set to h0 → tau+, tau- (how can the h_0 decay)

The entire LHC.in input file can be found attached at the end of this thesis. In the following chapters, a brief explanation for each of the given selections is made.

4.3.2 Luminosity

Luminosity is the ratio of detected events per unit area per unit time. As this event is a computational simulation, it is possible to manually set any desired value. Higher luminosity gives more data for jet reconstruction but also increases simulated noise, if present, and removes the simulation further from experimental results. If the luminosity is chosen magnitudes of size larger than any achievable one, while this may result in excellent jet reconstruction, the entire event becomes unfalsifiable and thus unusable.

4.3.3 OrderinAlpha

The OrderinAlpha controls the ordering of the strong coupling constant $alpha_s$ in the shower. The value of OrderingAlpha affects the accuracy of the simulation, with higher values resulting in greater accuracy. However, using higher values also increases the computational cost of the simulation.

4.3.4 Process

For the sake of simplifyng the simulation and avoiding unwanted noise, the only allowed process was the creation of two jets and a Higgs boson through proton proton collision. Thus, the expected $\phi\eta$ plot should contain cones at diametrically opposed quarters and an additional cone in the centre, corresponding to the two jets and Higgs boson.

4.3.5 Jet Selection

Jet regions are defined as the partitions of the detector, in which particles may be combined into a jet. The criteria can vary for each region but typically transverse momentum and radius are used.

4.3.6 Decay Modes

In the process used for this thesis, the decay of the Higgs boson was restricted to a tauon and an anti tauon for the sake of simplifying the diagrams and analysis. The program used as a basis for the loop calculations is the one from [7].

4.3.7 Run File

This file contains the commands to run the previously generated file, with an additional option to specify the amount of events that should be generated for this particular run. If no number is given, the default value of events is generated. If specified, an analysis scheme is automatically run through the event simulation output. This requires at least 100 events to be able to analyze data and at least 1e+4 to properly separate the analysed data from noise. Again, higher values give better results at the cost of higher computation time.

4.3.8 Postprocessing

After the simulation itself finished and was analyzed, it is possible to create graphical depictions of the output data for visual interpretation. In this thesis the Herwig built-in Rivet toolkit is used for the generation of histograms with statistical error bars. With rivet it is possible to plot the results of multiple Herwig runs with differing parameters against each other in one image, by specifying the directories in question. The results of events with the same coupling strength between the Higgs and V boson, but different values for FMSA are then visually compared.

4.3.9 Handler = NULL

Setting a Handler to NULL turns off the corresponding process during event generation. To simplify the simulation, both multi parton interactions and hadronization were turned off for the event generation.

4.4 Herwig usage in the scope of this thesis

Specifically, for the scope of this project, an LHC.in input file was written by Simon Plaetzer [16].
The following selection parameters were set in the input file: A fixed scale of 80 GeV for the matrix elements, a minimum of 15 GeV for the transverse momentum of the first and second jet and a cone radius of 0.4.
Using the LHC.in as well as batch scripts a version of the input file was created in a new folder for any variation of values for the various κ_Z, κ_W and FMSA values. A coupling to Z and W of 1 corresponds to the SM, while the current hypothesis as of march 2023 takes FMSA = 0. Herwig was then used to create a simulation of events with these constraints using Monte-Carlo integration. Afterwards, the created data was compared to the one from an LHC experiment to check whether the simulation with modified coupling constants and FMS factor would be a better fit to experimental data than the current version without such modifications. [4]

4.5 FMSA factor in Herwig

If the numerical value of the Higgs mass is given, then the couplings of the Higgs boson to any other particle (including itself) may no longer be treated as a free parameter in the SM. To search for small deviations from SM predictions or find alternative models, one can add new terms to the Lagrangian, called "anomalous couplings". These may not only influence the absolute value of a coupling, but also its underlying tensor structure. [12]
A form factor is a matrix element correction factor used to improve the description of multi-jet final states in hadronic collisions. With the Four-momentum transfer being $\mathcal{Q}^2$, it is a common practice, to multiply $\mathcal{Q}$ by a so called form factor, in order to include effects of higher order interaction terms. A form factor of one corresponds to no additional effects being included, the further it deviates the more interaction terms are included. [10]
According to a study done by CERN in 2021, the scattering amplitude between a h_0 and two V bosons is described by:

$$A(h_0 \to V_1 V_2) = \frac{1}{v}\left[a_1^{VV} + \frac{\kappa_1^{VV} q_{V1}^2 + \kappa_2^{VV} q_{V2}^2}{\left(\Lambda_1^{VV}\right)^2)}\right] \tag{2}$$

with q_{Vi} as four-momentum, $i = 1$ or 2 denoting the gauge boson, v as vacuum expectation value of h_0, Λ_0, Λ_1 constants (scales required in BSM to keep the κ_i^{VV} dimensionless) and a_1^{VV} as real number that modifies its corresponding amplitude term. For symmetry reasons, $\kappa_1^{VV} = \kappa_2^{VV}$. In general, at the tree level, only $a_1^{VV} \neq 0$ [1].
In this thesis the simplified version eq. (2) of the general expression given in [1] was used. Further, as mentioned in the beginning, to account for a non-zero radius of the bosons, the form factor was modified by the FMSA factor. This modification was included in the code as:

- double M = c.bosonMass/amplitudeScale();
- double Gamma = c.bosonWidth/amplitudeScale();
- double fij = fabs(1-Qij.m2()/sqr(M))+Gamma/M;
- double fkl = fabs(1-Qkl.m2()/sqr(M))+Gamma/M;
- double Mh = getParticleData(ParticleID::h0)-¿mass()/amplitudeScale();;
- double Gammah = getParticleData(ParticleID::h0)-¿mass()/amplitudeScale();;
- double fh = fabs(1-(Qij+Qkl).m2()/sqr(Mh))+Gammah/Mh;
- double FF = 1.+theFMSA*pow(fij*fkl*fh,-1./3.);

For comparison with eq. (2) a formulaic description of the Amplitude in Herwig is:

$$A(h_0 \to V_1 V_2) = \frac{A_s}{P_{ij} P_{kl}} \left[1 + a * \left(\left[\left| \frac{1 - m_{ij}}{\sqrt{M}} \right| + \frac{\Gamma}{\sqrt{M}} \right] * \left[\left| \frac{1 - m_{kl}}{\sqrt{M}} \right| + \frac{\Gamma}{\sqrt{M}} \right] * \left[\left| \frac{1 - m_{ij} - m_{kl}}{\sqrt{M}} \right| + \frac{\Gamma}{\sqrt{M}} \right] \right)^{-\frac{1}{3}} \right] \quad (3)$$

The value of the FMSA factor (theFMSA in the code above) is then, in simplified terms, a measure of how the value of the physical radius impacts the decay.
The parton shower produced by the CascadeHandler initially provides an approximation to the underlying physics up to the leading-order. The modification to the perturbative QCD matrix elements for multi-jet production is then modified by the APT term stemming from the radii of our bosons, divided by terms stemming from the invariant masses of the Higgs particle and two resulting jets. The so called "bosonFactor" result, which sets the coupling between Higgs and V is finally modified by a multiplication with the form factor (FF) gained by incorporating the FMSA adaption. The SM result is recovered by setting FMSA = 0.

5 Jet algorithms

Jets are the experimental signature of gluons and quarks, created in high energy interactions, eg. pp collisions. As gluons and quarks have net colour charge, they cannot exist freely due to colour confinement, instead bundling together to form net neutral clusters (jets). These clusters, called hadrons, are created by the process of hadronization.

5.1 Relativity

Before describing jet algorithms, the following list names the relativistic terminology used while discussing the jets.

- $Q^2 = (\vec{p_i} - \vec{p_f})^2 - (\vec{E_i} - \vec{E_f})^2$
- Q^2 in elastic scattering ... $2 \times M_T \times \Delta E$ (generally: square of transferred 4-Momentum)
- M_T ... target mass
- y ... rapidity
- η ... pseudorapidity
- m_{jj} ... Lorentz-invariant mass (colloquially 4-mass)
- p_T ... transverse momentum

[15]

Jets provide troves of information about physics within and beyond the standard model of particle physics. On the one hand, jets display the behavior of Quantum Chromodynamics (QCD) over a wide range of energy scales, from the energy of the hard scattering, through intermediate scales of branching and showering, to the lowest scale of hadronization. On the other hand, jets contain signatures of exotic physics when produced by the decays of heavy, strongly-interacting particles such as top quarks or particles beyond the Standard Model. [11]

5.2 IRC safety

IRC safety is a necessary constraint for ideal jet finding algorithms. This is based on the fact that one would expect the shape of jets to be conserved even when collinear splitting of the thus far hardest particle (often used as "seed" for jet construction) occurs. Additionally the jet shape should not be affected (or at least not be affected strongly) by soft radiation changing the energy of the jet, or the emission of a particle through soft decay changing the direction of the jet structure (ideally a cone). Of note is, too, that a jet as defined initially does not necessarily need to have the shape commonly associated with this term (ie. conical), as events triggered by the energy and momentum of the jet may very well lead to sub-jets, which have different directions. In a jet finding algorithm, which should help reconfigure the original event form, a conical shape of the original jet is still a good sign of the algorithm working as intended, as it could show the algorithm managed to filter out noise from these subjets.[3]

5.2.1 Introduction of the anti-kt algorithm

The data for this thesis was created with the anti-kt jet finding algorithm, which solves some issues regarding infrared and collinear splitting safety introduced by the kt and Aachen algorithm. The Aachen and kt- algorithm are sequential recombination algorithms, parameterized by the energy scale used for distance definition. The anti-kt algorithm was developed by first generalizing the concepts of distance between particles and adapting a general parameter p, which helps in uniting both the kt algorithm and Cambridge/Aachen algorithm into one formula:

$$d_{ij} = min(k_{ti}^{2p}, k_{tj}^{2p}) \frac{\Delta_{ij}^2}{R^2} \tag{4}$$

$d_{iB} = k_{ti}^{2p}$
$\Delta_{ij} = (y_i - y_j)^2 + (\Phi_i - \Phi_j)^2$
y_i = rapity
k_{ti} = transverse momentum
Φ_i = azimuth angle

Setting p = 1 leads to the kt, setting p = 0 to the Aachen algorithm. Choosing this newly identified parameter to be p = -1 will now lead to the anti-kt algorithm. [6]

5.2.2 General Behaviour of the anti-kt algorithm

Functionally, within the anti-kt algorithm, soft particles will first cluster around hard ones before merging with each other. On the other hand hard particles will absorb any soft particles within the radii 2R.
The jet radius R is a normalisation constant:

$$d_{li} = min\left(\frac{1}{k_{tl}^2}, \frac{1}{k_{ti}^2}\right) \frac{\Delta_{li}^2}{R^2} \tag{5}$$

These particles will only be absorbed if there are no other hard particles inside that radius. If another particle is found outside of R but inside of 2R, the shape of the final resulting jet depends on the transverse momenta of both hard particles, with the particle of higher k_t being granted more "area" of the two overlapping ones. Should the transverse momenta be roughly equal, the area shared between their cones will be clipped at the center of the overlap, resulting in two non-conical jets. Should both hard particles lie closer than R to each other, they will instead be merged (the center of this newly created singular hard particle will be shifted depending on the value of either original seeds transverse momentum). Again, this will result in conical jets unless k_{t1} k_{t2}. Thus the jets crated with anti-kt are resilient towards modification by soft particles but flexible towards hard radiation [6]. This conical behavior is the one naively expected of particles after a collision. However, in particle physics and relativity just such intuitive expectations are often proven flawed, as they are based on experiences from everyday life, which lie at the very boundary of either effect (too large to observe quantum mechanical effects and too low in energy to directly experience relativistic effects, although one can observe such effects and even measure them with finely tuned devices).
Considering the idea of jet shapes from a mathematical or physical perspective, one arrives at the same conical, distribution as the isotropic nature of space dictates there should not be any preferred direction, barring outside fields. Of course, this might clash with spontaneous symmetry breaking which, at the baseline, corresponds to a space-time which is no longer completely indistinguishable in any direction.

[3] this is in no way a criteria by which to judge the algorithm itself but rather an additional check after the algorithm has been proven to work well in theory and experiment.

Additionally, the invariant angular distribution is given only in the relativistic center of momentum system frame and thus must be Lorentz-shifted in order to compare it with events as observed in the laboratory frame of reference.

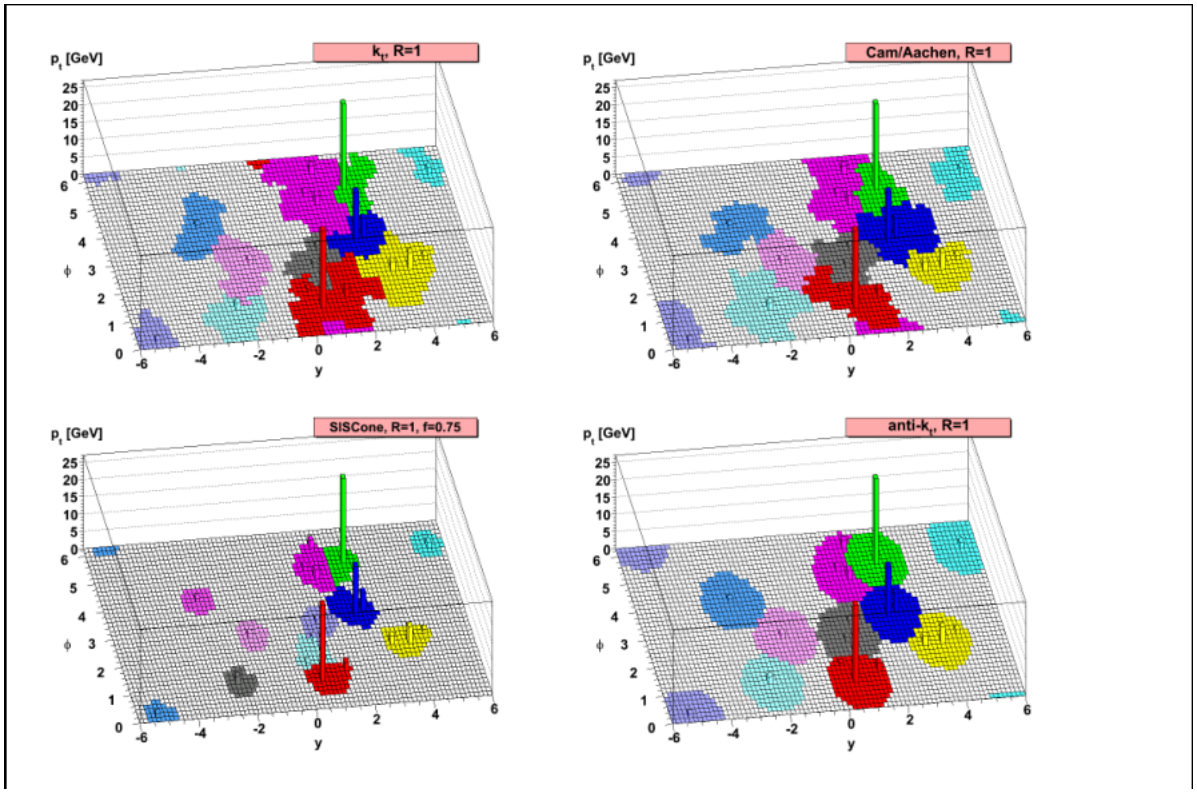

Fig. 6: A sample parton-level event (generated with Herwig), together with many random soft "ghosts", clustered with four different jet algorithms, illustrating the "active" catchment areas of the resulting hard jets. For k_t and Cam/Aachen the detailed shapes are in part determined by the specific set of ghosts used, and change when the ghosts are modified. image source : [6]

6 Simulation Results

The images generated by the simulation analysis part of Herwig (rivet-mkhtml) were then visually compared and any apparent distinctions from the regular graph course noted down. Initially large variations of these parameters were used, to find general changes in the jet behaviour. Once the effects of varying the parameters were known, in the following simulations the variation of the FMSA parameter was iteratively set over smaller values, until a cutoff point was found. Setting the FMSA value below this cutoff point, resulted in effects of such a small scale, they could not be separated from uncertainty. At and above the scale, the effects were still visible. In the following sections, an overview of the found effects of the FMSA parameter are given. The event result change after a variation of the SM couplings is compared against these effects as well. Any plots produced with rivet were plotted in natural units using either GeV or 1 as unit.

6.1 Overview

For the SM parameters κ_Z and κ_W, an increase in their normalisation value lead to more events occurring in their respective decay channels (higher $\frac{d\sigma}{d\Omega}$). The higher the coupling to either of those bosons, the more events were given by the simulation software. The correlation between coupling strength and event number was impacted more strongly by varying κ_w. This difference led to a ratio difference of $\mathcal{O}(1)$, which, while noticeable, did not effect a difference in the general graph structure.

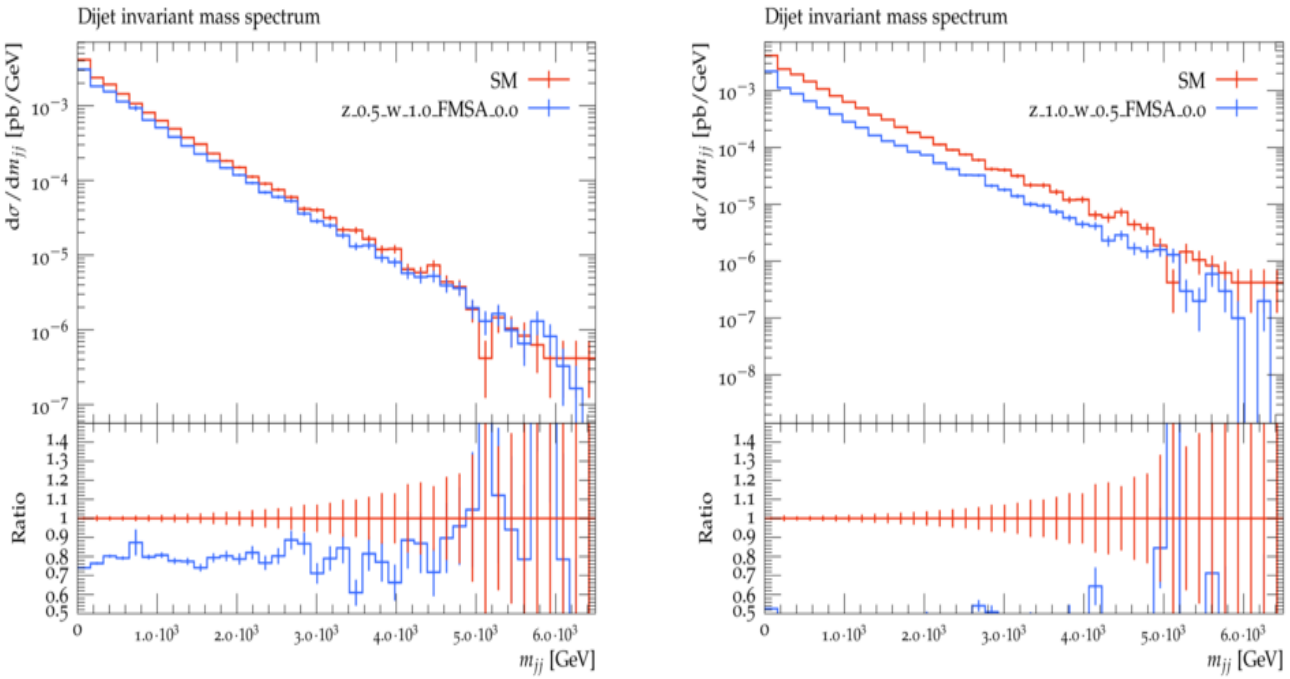

(a) m_{jj} for fixed κ_W (b) m_{jj} for fixed κ_Z

Fig. 7: difference in variation of κ_W and κ_Z

When setting FMSA to 10^{-3} or lower, the impact it has on the simulation results is not immediately obvious. At those stages, the effect of our κ_Z and κ_W variations are still of comparable impact. The composite value $\frac{\kappa_Z+\kappa_W}{2}$, which we will call ζ_κ is sufficient for a rough comparison of the general effect that FMSA has. Keeping in mind, that κ_W effects the event number more strongly, both options (fixed κ_Z or fixed κ_W) will be compared separately if necessary. In the SM, used as reference, $\zeta = \zeta_{SM} = 1$.
The effect of FMSA was shown more clearly when setting it to 0.5 or 1.0. The value of ζ is no longer the only measure of deviation from the SM plot. Instead, a new value $\bar{\zeta} = \zeta + FMSA$ is a better measure of how well the plots correspond to the SM one. Thus it appears that FMSA raises the amount of events detected linearily.

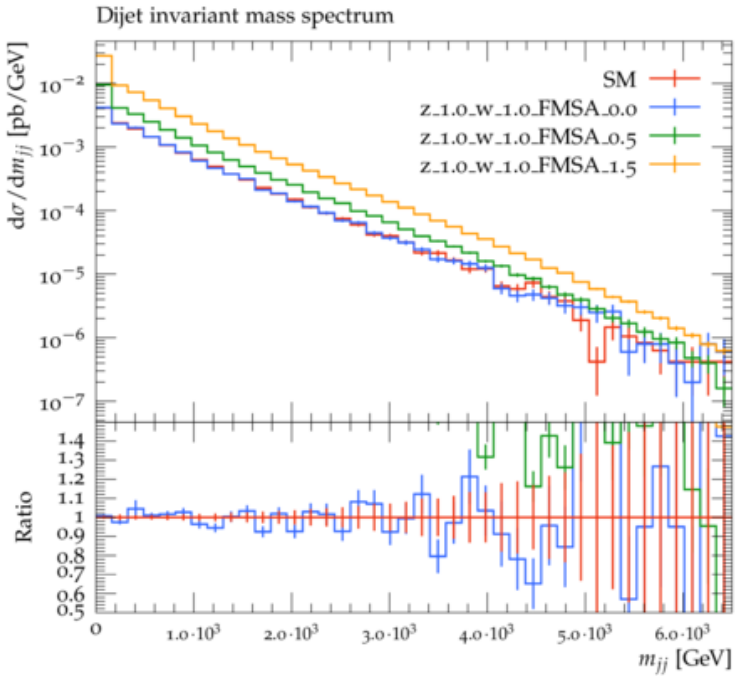

Fig. 8: effect of varying FMSA

6.2 Rough Search

The initial simulations were aimed at finding an effect introduced by FMSA as well as checking if such an effect would differ from simply varying the V boson coupling. The amount of events selected (N_e), which suppresses structures caused random events towards the general graph shape, was chosen to be 10^5 for the rough grid search due to simulation time constraints.
Initially, the variations of κ_Z, κ_W and FMSA were checked against each other. When comparing how the differential cross section changed in response to the variations, at first glance it behaved the same for changing either the FMSA parameter or the SM coupling strength (fig. 7 and fig. 8). However, when comparing transverse momentum dependant values, it became apparent, that the FMSA effect no longer led to the same changes at large GeV values (section 6.2 and fig. 10). This change was only noticeable in p_T-dependant values, as fig. 11 shows that there was no angular dependance (similarly, independance on η, y and any other non-p_T value was seen).

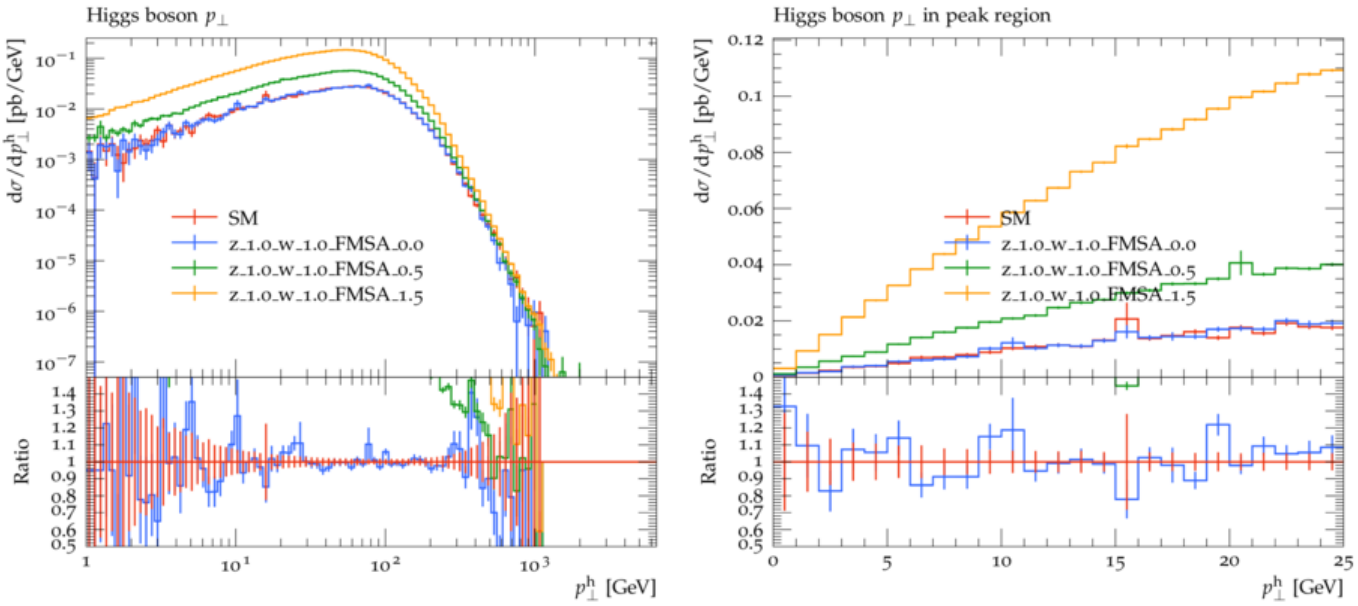

(a) p_T for varying κ_z (b) p_T for varying κ_z

Fig. 9: effect of varying the SM coupling strength

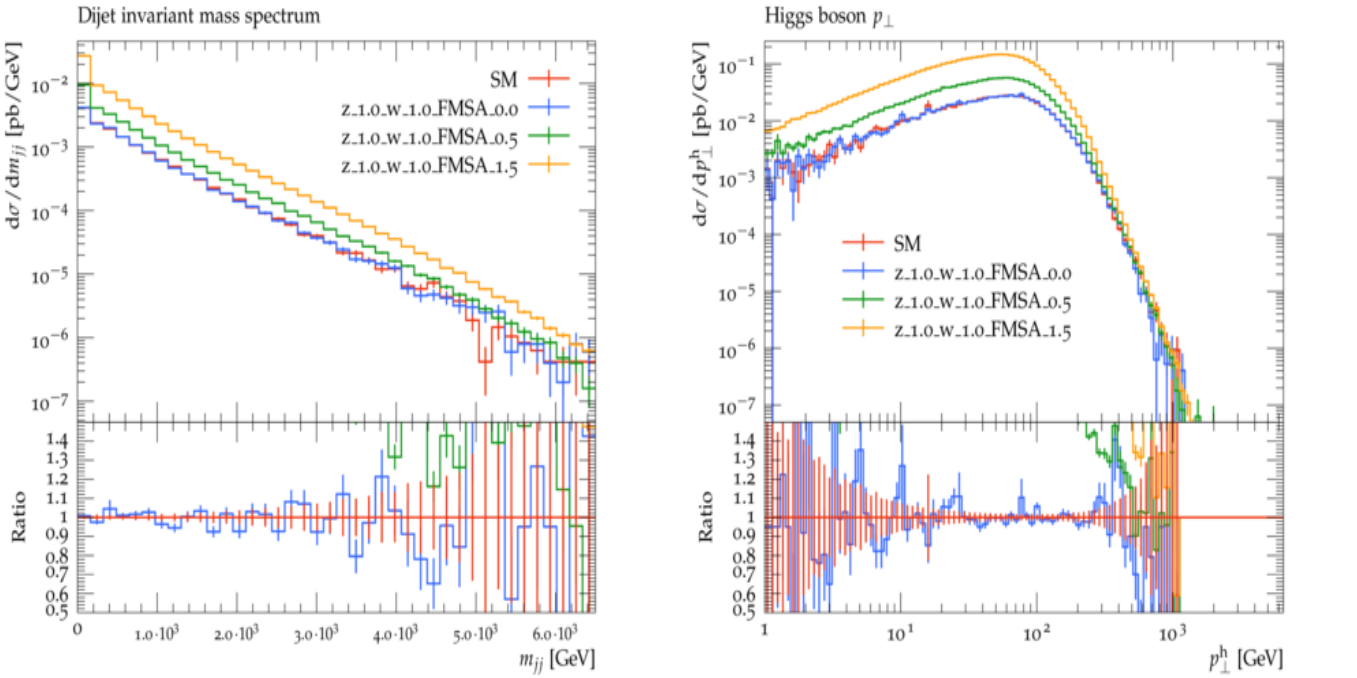

Fig. 10: Dropoff for transverse momenta of jets

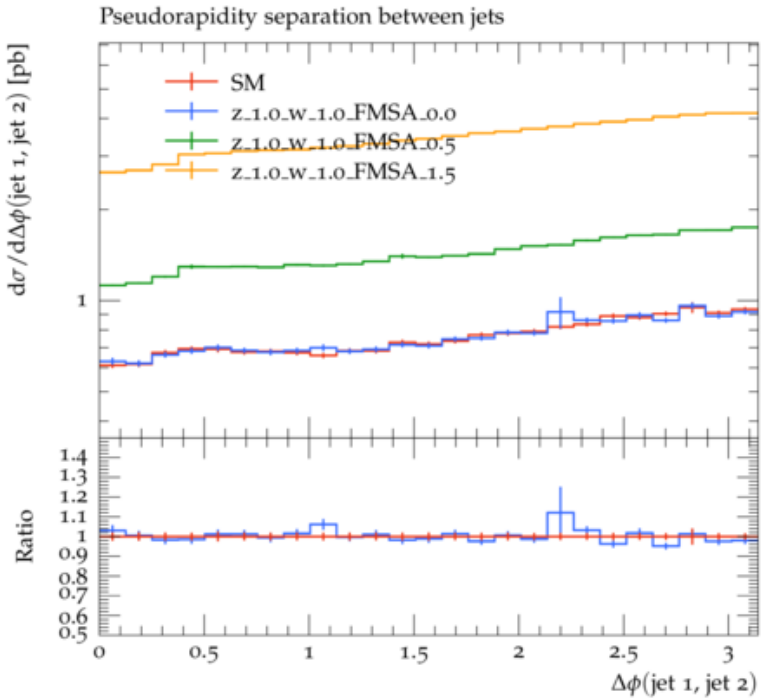

Fig. 11: effect of varying the anomalous coupling strength. No angular dependance

6.3 Fine Search

After finding the effect mentioned in section 6.2, the grid spacing was lessened in iterations to find the value of FMSA after which the difference could clearly be seen in the generated graphs. N_e was set to 10^7 for the fine search. For this N_e, the cutoff value at which the FMSA-modified plot was still distinguishable from the SM and the dropoff at high p_T was still visible was taken to be 0.03. As seen in fig. 12a, the difference, while not visible on the logarithmic scaled (upper image part) was still visible for the ratio plot (lower image part). For the selected N_e, the ratio was already not always separable from uncertainty (fig. 12b). For the leptons (fig. 12c) the difference was still visible, but the high p_T drop-off already hidden within uncertainty oscillations. For jets (fig. 12d) the drop-off was still visible, but at lower values even this was swallowed up by uncertainty.

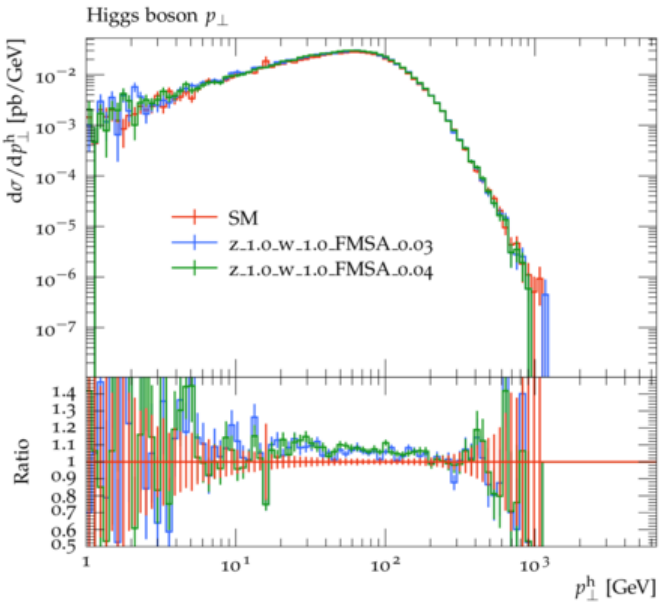

(a) Higgs p_T

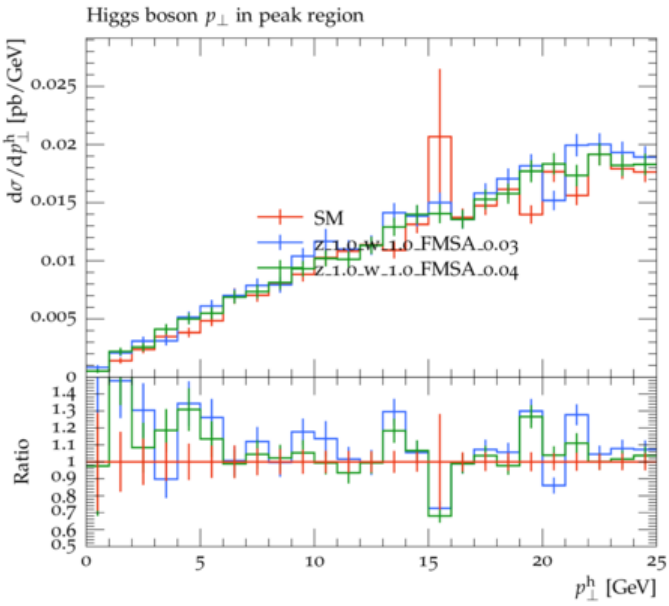

(b) Higgs p_T in the peak region

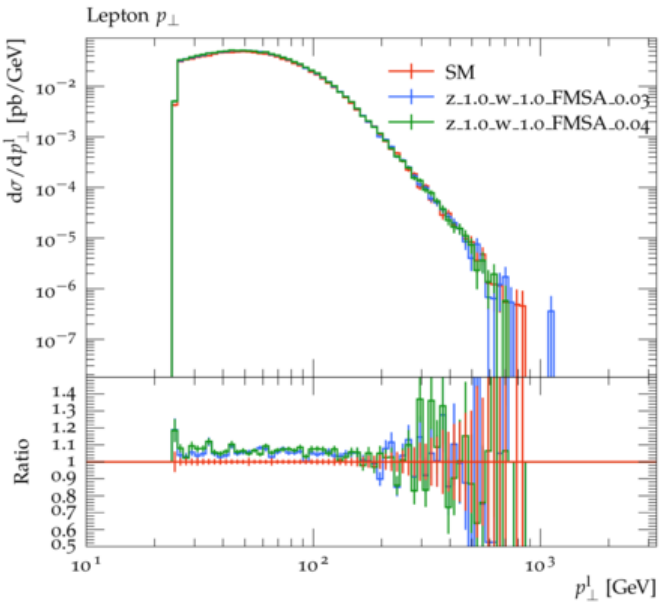

(c) lepton p_T

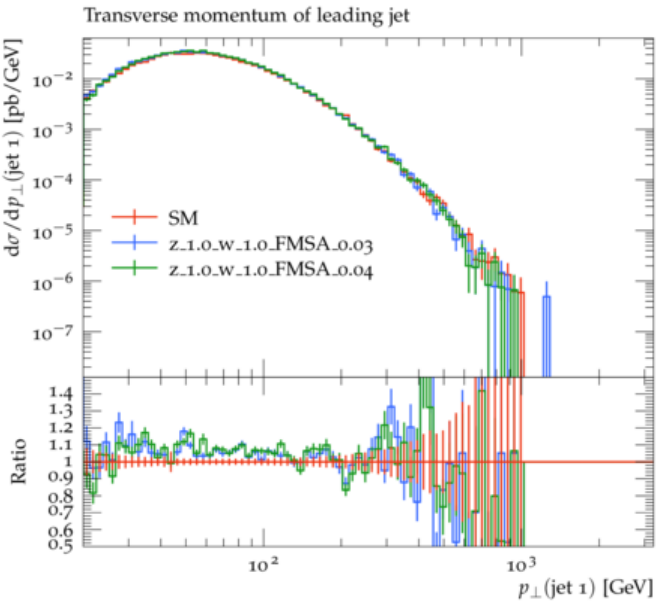

(d) jet p_T

Fig. 12: cutoff value for 10^7 events

While the cutoff value is already on the verge of showing all effects, in comparison with previous (rough estimate) runs, it can be seen that the increase in the differential cross section for higher FMSA values is of comparable impact as the result of raising SM couplings in a loew p_T regime (up to 300 GeV) and seems to vanish at high p_T (above 500 GeV).

7 Discussion and Outlook

7.1 Summary

In this thesis the effect of changing the coupling between h_0 and a V boson was studied. For this purpose the Herwig event generator was used, along with some simplifications: Setting the decay channel to $h_0 \to \tau^+\tau^-$, setting the tauons as stable (non-decaying) particles, the h_0 mass to 125 GeV and only calculating the Matrix elements up to a linear order. Furthermore, to simplify the simulation, multi parton interactions and hadronization were turned off for the

event generation.
To test BSM effects, a perturbation was added into the form factor, affecting the matrix element. This perturbation, FMSA, represents anomalous coupling resulting from giving bosons a non-zero radius. It was then visible, that For this purpose, the "bosonFactor" function used in the HJets library was modified by multiplication with this form factor. Initially, the coupling between h_0 and one of the V bosons as well as the FMSA factor were varied individually and the resulting $\frac{d\sigma}{d\Omega}$ compared. Thus it was found, that both variations result in a similar change in the differential cross section at most plots. When comparing the transverse momentum of the jets however, the observed change by adding FMSA ≥ 0 was no longer visible. It can then be said, that the two ideas (varying the FMSA parameter and varying the SM coupling) achieve different cross sections.
The event flow response to these three variations was compared, so the following differences and similarities were noted:

- The variation of SM coupling had the same general result for κ_Z and κ_W.
- The variation of κ_W had a stronger response to varying it by the same numerical value as κ_Z.
- Varying FMSA lead to a similar change in event flow response as the couplings. However, at large p_T values, this effect vanished

The anomalous coupling effect was noticeable while FMSA ≥ 0.03 for 10^7 events. It can also be seen, that a modification of $\zeta \to \zeta' = \zeta +$ FMSA is visible. Meaning FMSA recovers some regular coupling strength at low GeV values.

7.2 Future Outlook

Before moving on to more involved simulations and calculations, it is first necessary to check whether the noted effect is retained after de-simplifying the simulation. Thus the first logical step would be to run a more complete simulation, including parton interactions, hadronization as well as Matrix elements of next-to-leading-order and beyond. A larger event size might also prove useful to further refine the current estimation of the FMSA value, after which the effect becomes noticeable.
Should those simulations still give similar results as this thesis, next steps could include adapting the SM formulas to this small perturbation, finding which experiments or values would further be affected by this change and comparing the data available for those. If the calculations and simulations still show the p_T dependant effect, one could then go on to construct an experimental setup or measurement technique to further probe this regime.

8 code

```
    # -*- ThePEG-repository -*-

##################################################
## Herwig/Matchbox example input file
##################################################

##################################################
## Collider type
##################################################
read snippets/Matchbox.in
read snippets/PPCollider.in

##################################################
## Beam energy sqrt(s)
##################################################

cd /Herwig/EventHandlers
set EventHandler:LuminosityFunction:Energy 13000*GeV

##################################################
## Process selection
##################################################
```

```
## Note that event generation may fail if no matching matrix element has
## been found.  Coupling orders are with respect to the Born process,
## i.e. NLO QCD does not require an additional power of alphas.

## Model assumptions
read Matchbox/StandardModelLike.in
read Matchbox/DiagonalCKM.in

## Set the order of the couplings
cd /Herwig/MatrixElements/Matchbox
set Factory:OrderInAlphaS 0
set Factory:OrderInAlphaEW 3

## Select the process
## You may use identifiers such as p, pbar, j, l, mu+, h0 etc.
do Factory:Process p p -> j j h0

## Special settings required for on-shell production of unstable particles
## enable for on-shell top production
# read Matchbox/OnShellTopProduction.in
## enable for on-shell W, Z or h production
# read Matchbox/OnShellWProduction.in
# read Matchbox/OnShellZProduction.in
 read Matchbox/OnShellHProduction.in
# Special settings for the VBF approximation
# read Matchbox/VBFDiagramsOnly.in

######################################################
## Matrix element library selection
######################################################

## Select a generic tree/loop combination or a
## specialized NLO package

# read Matchbox/MadGraph-GoSam.in
# read Matchbox/MadGraph-MadGraph.in
# read Matchbox/MadGraph-NJet.in
# read Matchbox/MadGraph-OpenLoops.in
 read Matchbox/HJets.in
# read Matchbox/VBFNLO.in

## Uncomment this to use ggh effective couplings
## currently only supported by MadGraph-GoSam

# read Matchbox/HiggsEffective.in

######################################################
## Cut selection
## See the documentation for more options
######################################################
cd /Herwig/Cuts/
#set ChargedLeptonPairMassCut:MinMass 60*GeV
#set ChargedLeptonPairMassCut:MaxMass 120*GeV

## cuts on additional jets

read Matchbox/DefaultPPJets.in
```

```
insert JetCuts:JetRegions 0 FirstJet
insert JetCuts:JetRegions 1 SecondJet
# insert JetCuts:JetRegions 2 ThirdJet
# insert JetCuts:JetRegions 3 FourthJet

##################################################
## Scale choice
## See the documentation for more options
##################################################

cd /Herwig/MatrixElements/Matchbox
set Factory:ScaleChoice /Herwig/MatrixElements/Matchbox/Scales/HTScale

##################################################
## Matching and shower selection
## Please also see flavour scheme settings
## towards the end of the input file.
##################################################

# read Matchbox/MCatNLO-DefaultShower.in
# read Matchbox/Powheg-DefaultShower.in
## use for strict LO/NLO comparisons
read Matchbox/MCatLO-DefaultShower.in
## use for improved LO showering
# read Matchbox/LO-DefaultShower.in

# read Matchbox/MCatNLO-DipoleShower.in
# read Matchbox/Powheg-DipoleShower.in
## use for strict LO/NLO comparisons
# read Matchbox/MCatLO-DipoleShower.in
## use for improved LO showering
# read Matchbox/LO-DipoleShower.in

# read Matchbox/NLO-NoShower.in
# read Matchbox/LO-NoShower.in

##################################################
## Scale uncertainties
##################################################

# read Matchbox/MuDown.in
# read Matchbox/MuUp.in

##################################################
## Shower scale uncertainties
##################################################

# read Matchbox/MuQDown.in
# read Matchbox/MuQUp.in

##################################################
## PDF choice
##################################################

read Matchbox/FiveFlavourScheme.in
## required for dipole shower and fixed order in five flavour scheme
```

```
# read Matchbox/FiveFlavourNoBMassScheme.in
read Matchbox/CT14.in
# read Matchbox/MMHT2014.in

####################
#manual additions
########################

do /Herwig/Particles/h0:SelectDecayModes h0->tau-,tau+;
set /Herwig/Shower/ShowerHandler:MPIHandler NULL
set /Herwig/EventHandlers/EventHandler:HadronizationHandler NULL
set /Herwig/Particles/tau+:Stable Stable
set /Herwig/Particles/tau-:Stable Stable

set /Herwig/MatrixElements/Matchbox/Amplitudes/HJets/Amplitudehqqbarkkbar:KappaZ 1.0
set /Herwig/MatrixElements/Matchbox/Amplitudes/HJets/Amplitudehqqbarkkbar:KappaW 1.0
set /Herwig/MatrixElements/Matchbox/Amplitudes/HJets/Amplitudehqqbarkkbar:FMSA 0.0
set /Herwig/Analysis/Basics:CheckQuark No

##################################################
## Analyses
##################################################

cd /Herwig/Analysis
insert Rivet:Analyses 0 MC_HJETS
insert Rivet:Analyses 0 MC_HINC
insert /Herwig/Generators/EventGenerator:AnalysisHandlers 0 Rivet
insert /Herwig/Generators/EventGenerator:AnalysisHandlers 0 HepMC

##################################################
## Save the generator
##################################################

do /Herwig/MatrixElements/Matchbox/Factory:ProductionMode


cd /Herwig/Generators
saverun LHC-Matchbox EventGenerator
```

[16]

9 References

References

[1] A.M. Sirunyan et al. "Constraints on anomalous Higgs boson couplings to vector bosons and fermions in its production and decay using the four-lepton final state". In: *Physical Review D* 104.5 (Feb. 2021). DOI: 10.1103/physrevd.104.052004. URL: https://doi.org/10.1103%2Fphysrevd.104.052004.

[2] G. Aad et al. "Measurements of the Higgs boson production and decay rates and coupling strengths using pp collision data at \sqrt{s}=7 s = 7 and 8 TeV in the ATLAS experiment". In: *The European Physical Journal C* 76.1 (Jan. 2016). DOI: 10.1140/epjc/s10052-015-3769-y. URL: https://doi.org/10.1140%2Fepjc%2Fs10052-015-3769-y.

[3] A.M. Sirunyan et. al. "Observation of the Higgs boson decay to a pair of leptons with the CMS detector". In: *Physics Letters B* 779 (Apr. 2018), pp. 283–316. DOI: 10.1016/j.physletb.2018.02.004. URL: https://doi.org/10.1016%2Fj.physletb.2018.02.004.

[4] Johannes Bellm et al. "Herwig 7.2 Release Note". In: *The European Physical Journal C* 80.5 (May 2020), p. 452. ISSN: 1434-6044, 1434-6052. DOI: 10.1140/epjc/s10052-020-8011-x. arXiv: 1912.06509[hep-ph]. URL: http://arxiv.org/abs/1912.06509 (visited on 04/30/2023).

[5] Christian Bierlich et al. "Robust Independent Validation of Experiment and Theory: Rivet version 3". In: *SciPost Physics* 8.2 (Feb. 2020). DOI: 10.21468/scipostphys.8.2.026. URL: https://doi.org/10.21468%2Fscipostphys.8.2.026.

[6] Matteo Cacciari, Gavin P. Salam, and Gregory Soyez. "The anti-k_t jet clustering algorithm". In: *Journal of High Energy Physics* 2008.4 (Apr. 16, 2008), pp. 063–063. ISSN: 1029-8479. DOI: 10.1088/1126-6708/2008/04/063. arXiv: 0802.1189[hep-ph]. URL: http://arxiv.org/abs/0802.1189 (visited on 04/30/2023).

[7] Francisco Campanario et al. "Electroweak Higgs Boson Plus Three Jet Production at Next-to-Leading-Order QCD". In: *Phys. Rev. Lett.* 111 (21 Nov. 2013), p. 211802. DOI: 10.1103/PhysRevLett.111.211802. URL: https://link.aps.org/doi/10.1103/PhysRevLett.111.211802.

[8] *CERN experiments observe particle consistent with long-sought Higgs boson — CERN*. URL: https://home.cern/news/press-release/cern/cern-experiments-observe-particle-consistent-long-sought-higgs-boson (visited on 04/30/2023).

[9] Markus Cristinziani and Martijn Mulders. "Top-quark physics at the Large Hadron Collider". In: *Journal of Physics G: Nuclear and Particle Physics* 44.6 (June 1, 2017), p. 063001. ISSN: 0954-3899, 1361-6471. DOI: 10.1088/1361-6471/44/6/063001. URL: https://iopscience.iop.org/article/10.1088/1361-6471/44/6/063001 (visited on 04/30/2023).

[10] B. Desplanques and Y. B. Dong. *Form factors in relativistic quantum mechanics: constraints from space-time translations*. 2008. arXiv: 0810.2386 [nucl-th].

[11] Stephen D. Ellis et al. "Jet Shapes and Jet Algorithms in SCET". In: *Journal of High Energy Physics* 2010.11 (Nov. 2010), p. 101. ISSN: 1029-8479. DOI: 10.1007/JHEP11(2010)101. arXiv: 1001.0014[hep-ph]. URL: http://arxiv.org/abs/1001.0014 (visited on 04/30/2023).

[12] LHC Higgs Cross Section Working Group et al. *LHC HXSWG interim recommendations to explore the coupling structure of a Higgs-like particle*. 2012. arXiv: 1209.0040 [hep-ph].

[13] Peter W. Higgs. "Broken Symmetries and the Masses of Gauge Bosons". In: *Physical Review Letters* 13.16 (Oct. 19, 1964), pp. 508–509. ISSN: 0031-9007. DOI: 10.1103/PhysRevLett.13.508. URL: https://link.aps.org/doi/10.1103/PhysRevLett.13.508 (visited on 04/30/2023).

[14] *How did we discover the Higgs boson? — CERN*. URL: https://home.cern/science/physics/higgs-boson/how (visited on 04/30/2023).

[15] Timon Idema. "Mechanics and Relativity". In: (2018). Publisher: TU Delft Open. DOI: 10.5074/T.2018.002. URL: https://textbooks.open.tudelft.nl/index.php/textbooks/catalog/book/14 (visited on 04/30/2023).

[16] Simon plaetzer. *LHC.in HERWIG input fileas used in this thesis*. 2023.

[17] Raubitzek Sebastian. *The size of the W-boson*. URL: https://static.uni-graz.at/fileadmin/_Persoenliche_Webseite/maas_axel/raubitzek.pdf.

[18] *The Higgs boson — CERN*. URL: https://home.cern/science/physics/higgs-boson (visited on 04/30/2023).

[19] *What's so special about the Higgs boson? — CERN*. URL: https://home.cern/science/physics/higgs-boson/what (visited on 04/30/2023).

List of Figures